

# Top-down and bottom-up through-thickness current anisotropy in a bilayer $\text{YBa}_2\text{Cu}_3\text{O}_{7-x}$ film

Z. J. Chen,<sup>a)</sup> D. M. Feldmann,<sup>b)</sup> and D. C. Larbalestier<sup>a)</sup>  
*University of Wisconsin-Madison, Madison, Wisconsin 53706*

T. G. Holesinger  
*Los Alamos National Laboratory, Los Alamos, New Mexico 87545*

X. Li, W. Zhang, and M. W. Rupich  
*American Superconductor, 2 Technology Drive, Westborough, Massachusetts 01581*

(Received 1 May 2007; accepted 10 July 2007; published online 2 August 2007)

The authors find the critical current anisotropy of a bilayer  $\text{YBa}_2\text{Cu}_3\text{O}_{7-\delta}$  film with different pinning structures in each layer is the sum of the anisotropy of the two individual layers, revealing that it is possible to tune the anisotropy of the composite through variation of an individual layer's thickness and pinning structure.  $\text{YBa}_2\text{Cu}_4\text{O}_x$  intergrowths and  $\text{Dy}_2\text{O}_3$  nanodots were the dominant pinning structures in the top and bottom layers, respectively. The bottom layer of the composite was isolated using traditional  $\text{Ar}^+$  ion milling and the top layer was isolated using a focused ion beam, allowing each layer to be studied independently. © 2007 American Institute of Physics.

[DOI: 10.1063/1.2767772]

High temperature superconducting (HTS) materials and wires hold enormous promise for the efficient generation, transmission, storage, and end use of electric power.<sup>1</sup> The critical current density ( $J_c$ ) is determined largely by nanoscale defect structures that pin vortices and hence prevent resistive current flow; however, defects that pin vortices at one field orientation or temperature are frequently different from those that support a high  $J_c$  elsewhere in field-temperature space.<sup>2,3</sup> Understanding the nature of pinning defects is critical to the synthesis of nanoengineered superconductors optimized for large  $J_c$  values over a wide range of temperatures and applied fields.

Stoichiometric  $\text{YBa}_2\text{Cu}_3\text{O}_{7-\delta}$  (YBCO) films usually have a high density of defects that may act as vortex pinning centers, including misfit dislocations,<sup>4</sup> edge and screw dislocations,<sup>5</sup> oxygen vacancies, impurity atoms, grain boundaries,<sup>6</sup> and stacking faults. Significant efforts have recently been made to improve pinning through additions or substitutions to the YBCO lattice in order to introduce additional pinning structures.<sup>2,7-10</sup> YBCO films grown by the *ex situ* trifluoroacetate-based metal organic deposition (MOD) process,<sup>11</sup> an industrially scalable process,<sup>12</sup> have a large number of  $\text{YBa}_2\text{Cu}_4\text{O}_y$  (Y124) intergrowths.<sup>13</sup> These intergrowths are believed to be responsible for greatly enhanced  $J_c$  for magnetic fields  $H$  applied along the  $ab$  planes ( $H\parallel ab$ ), and typically  $J_c(H\parallel ab)/J_c(H\parallel c) \sim 4$  at 65 K and 3 T.<sup>3</sup> Rare-earth oxide additions in such films tend to form randomly distributed, spherical rare-earth oxide particles within the YBCO lattice, with pronounced strain fields along the  $c$  axis<sup>14</sup> that lead to greatly improved  $J_c$  for  $H$  applied along the  $c$  axis ( $H\parallel c$ ).<sup>14-16</sup> However, the presence of rare-earth oxide particles greatly diminishes the number of Y124 intergrowths, and in such films typically  $J_c(H\parallel ab)/J_c(H\parallel c) \sim 1-2$  at 65 K and 3 T. Large numbers of both defect types

have not yet been produced in single layer MOD-grown films.<sup>14,15</sup>

The maximum strength of a magnetic field and the field orientation experienced by a YBCO wire are application dependent, underscoring the importance of the  $J_c$  anisotropy. In a typical solenoid of YBCO wire, wound with the plane of the wire parallel to the axial field, the highest magnetic field  $H\parallel ab$  experienced by the wire is approximately two times higher than for  $H\parallel c$ .<sup>17</sup> It is therefore desirable to be able to independently tune  $J_c(H\parallel c)$  and  $J_c(H\parallel ab)$  to meet this demand. As noted above, large densities of Y124 intergrowths and rare-earth oxides, capable of enhancing  $J_c(H\parallel c)$  and  $J_c(H\parallel ab)$ , respectively, are difficult to introduce into single layer MOD-grown films. This limitation was recently circumvented by depositing a bilayer YBCO film,<sup>17</sup> where each defect type described above is dominant in one layer. In this work, we examine the microstructure, self-field  $J_c$ , and in-field  $J_c$  anisotropy in such a film, in both the overall composite and in each layer individually.

The sample in this work employed a rolling assisted biaxially textured substrate<sup>18</sup> with an architecture of YBCO (1.75  $\mu\text{m}$ )/ $\text{CeO}_2$  (75 nm)/yttria-stabilized zirconia (75 nm)/ $\text{Y}_2\text{O}_3$  (75 nm)/Ni-5 wt. % (75  $\mu\text{m}$ ). The YBCO film was grown by MOD.<sup>11</sup> After solution deposition and decomposition of the first precursor layer, a second precursor layer was deposited and decomposed, and then the bilayer precursor was converted to YBCO. Further details are given elsewhere.<sup>12</sup> The composition of the precursors was such that the nominal stoichiometry of the resulting top and bottom YBCO layers was  $\text{YBa}_2\text{Cu}_3\text{O}_{7-\delta}$  and  $\text{YDy}_{0.5}\text{Ba}_2\text{Cu}_3\text{O}_{7-\delta}$ , respectively. The top layer contained a large number of Y124 intergrowths, and the Dy-doped bottom layer contained a large number of spherical rare-earth oxide particles, hereafter referred to as  $\text{Dy}_2\text{O}_3$  nanodots, though they are likely a mixture of Y and Dy ( $\text{Dy}_{2-y}\text{Y}_y\text{O}_3$ ). The thicknesses of the layers were 0.55 (top) and 1.2  $\mu\text{m}$  (bottom). For transport characterizations, a 250  $\mu\text{m}$  wide by 600  $\mu\text{m}$  long link was cut with a Nd-doped yttrium aluminium garnet laser. The measured  $J_c(0 \text{ T}, 77 \text{ K})$  and  $I_c(0 \text{ T}, 77 \text{ K})$  values were

<sup>a)</sup>Present address: National High Magnetic Field Laboratory, Florida State University, 2031 E. Paul Dirac Drive, Tallahassee, FL 32310.

<sup>b)</sup>Present address: Los Alamos National Laboratory, Los Alamos, NM 87545; electronic mail: dmfeldmann@lanl.gov

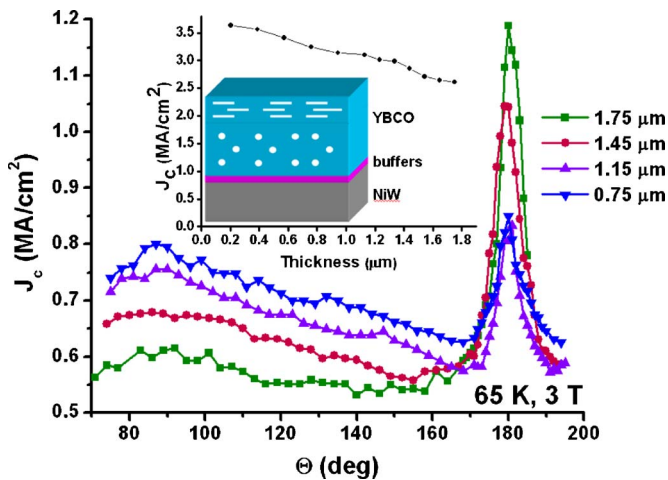


FIG. 1. (Color online) Angular dependence of  $J_c$  at 65 K and 3 T as a function of film thickness.  $90^\circ$  and  $180^\circ$  represent  $H$  applied along the  $c$  axis and  $ab$  axes of the YBCO film, respectively. The inset presents the self-field  $J_c(77\text{ K})$  as a function of film thickness as the film is thinned. The inset's inset shows a schematic of the bilayer film, with a pronounced density of Y124 intergrowths in the top and  $\text{Dy}_2\text{O}_3$  nanodots in the bottom.

$2.6\text{ MA/cm}^2$  and  $450\text{ A/cm}$  width, respectively. To study the transport properties through thickness, the film was successively thinned by ion milling and measured as described elsewhere.<sup>19</sup> At selected thicknesses,  $J_c$  was measured in magnetic fields  $H$  applied perpendicular to the direction of current flow and at an angle  $\Theta$  with the film surface. Isolation of the top half of the film was accomplished using a Zeiss 1540 focused ion beam (FIB). Transmission electron microscopy (TEM) images were taken on a Tecnai TF30 TEM/scanning TEM microscope operating at 300 kV.

Figure 1 presents  $J_c(\Theta)$  as a function of film thickness  $t$ . At full thickness ( $1.75\ \mu\text{m}$ ),  $J_c(H\parallel ab)/J_c(H\parallel c) \sim 2$ , which is only half the ratio typically found in single layer, nominally stoichiometric MOD-grown YBCO films (without rare-earth additions).<sup>3</sup> At full thickness the  $J_c$  anisotropy is influenced by both the Y124 intergrowths and the  $\text{Dy}_2\text{O}_3$  nanodots. As the film was thinned by  $\text{Ar}^+$  ion milling, the layer containing the high density of Y124 intergrowths was removed first until for the last two steps (1.15 and  $0.75\ \mu\text{m}$ ) only the  $\text{Dy}_2\text{O}_3$  nanodots remained. The effect is evident in the figure—the  $ab$ -plane peak (Y124 correlated pinning) decreases while the  $c$ -axis peak ( $\text{Dy}_2\text{O}_3$  correlated) increases. The  $J_c(\Theta, 65\text{ K}, 3\text{ T})$  curve for the last two steps strongly resembles similar curves for single layer rare-earth oxide doped films,<sup>16</sup> demonstrating that the  $\text{Dy}_2\text{O}_3$  particles have preserved their pinning properties in this bilayer film. The inset of Fig. 1 presents self-field  $J_c(77\text{ K})$  as a function of film thickness. The linear, monotonic increase in  $J_c$  as the film is milled indicates no dead layers and an overall very high  $J_c$ , and is similar to the thickness dependence observed for single-layer MOD-grown films.<sup>20,21</sup> The inset to the inset is a schematic of the film highlighting the dominant pinning structures.

Figure 2 presents cross sectional TEM images from the top (a) and the bottom (b) layers of the composite. The fine horizontal structures in Fig. 2(a) are the Y124 intergrowths within the YBCO lattice believed responsible for enhanced  $J_c(H\parallel ab)$ .<sup>3</sup> In Fig. 2(b) a high density of round  $\text{Dy}_2\text{O}_3$  particles is visible, and there is a distinct lack of Y124 intergrowths. The  $\text{Dy}_2\text{O}_3$  particles have been associated with en-

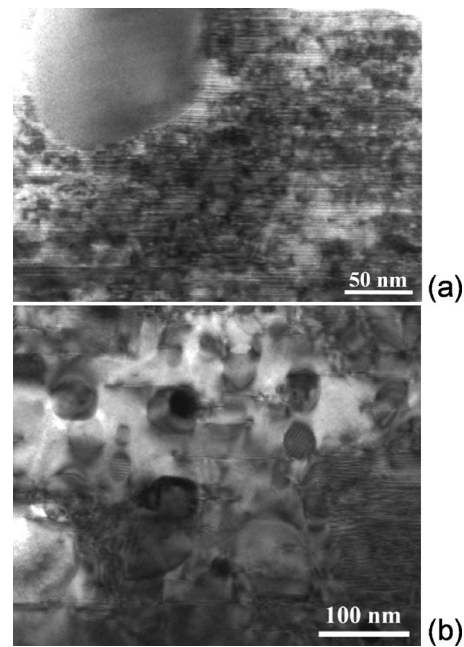


FIG. 2. Cross-sectional TEM images from (a) the top and (b) bottom layer of the bilayer film. A second phase particle is present in the upper left corner of (a). Extensive Y124 intergrowths are seen in (a), while round  $\text{Dy}_2\text{O}_3$  nanodots are evident in (b).

hanced  $J_c(H\parallel c)$ ,<sup>15,16</sup> and the lack of Y124 intergrowths reduces  $J_c(H\parallel ab)$ , as shown in Fig. 1.

Removal of the top layer revealed the pinning properties of the  $\text{Dy}_2\text{O}_3$  particles. To reveal the effects of the Y124 intergrowths, we removed the bottom layer of the film (containing the  $\text{Dy}_2\text{O}_3$  particles) with a FIB. We first cut a link  $1\ \mu\text{m}$  wide and  $2\ \mu\text{m}$  long, and then tilted the sample and removed the bottom  $1.2\ \mu\text{m}$  of the YBCO, leaving the “floating” link shown in Fig. 3.  $J_c(\Theta, 65\text{ K}, 3\text{ T})$  for this link is shown in Fig. 1, along with the isolated bottom layer. The difference between the two layers is striking, and a reflection of the dominant pinning mechanisms in each layer. For the bottom layer  $J_c(H\parallel ab)/J_c(H\parallel c) \sim 1$ , while for the top

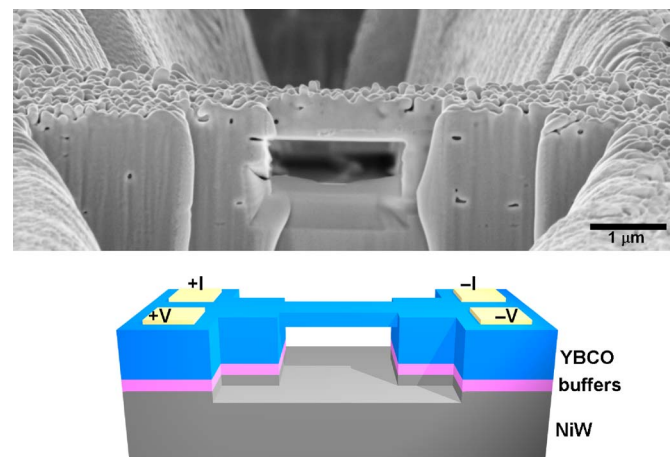


FIG. 3. (Color online) A SEM image (top) of the FIB-cut link that isolated the top layer of the YBCO film for transport measurement. The link was  $0.55\ \mu\text{m}$  thick and contained only the top layer of the bilayer composite. The majority of the cutting was done at a beam current of  $1\ \text{nA}$  to avoid heating the sample, and the total FIB milling time was  $\sim 20\ \text{h}$ . Below the SEM image is a schematic of the same link showing the geometry of the current and voltage pads.

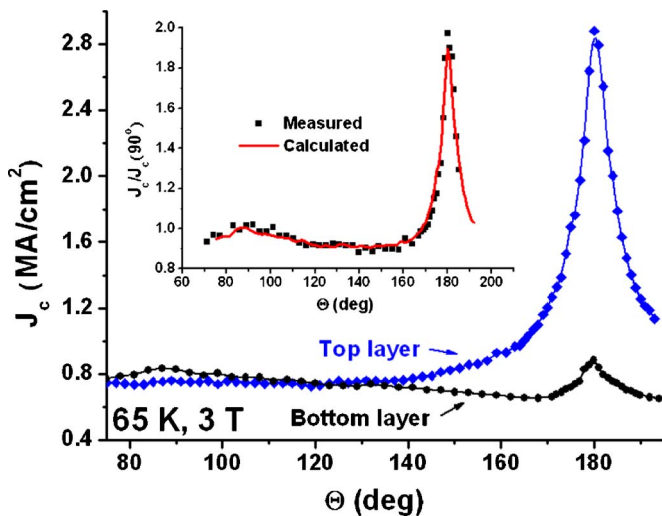


FIG. 4. (Color online) Angular dependence of  $J_c$  at 65 K and 3 T for the top and bottom layers of the composite individually. The inset presents normalized  $J_c(\theta, 65 \text{ K}, 3 \text{ T})$  for the full film thickness as measured and as calculated from the thickness-weighted sum of the individual layers  $[0.55/1.75J_c^{\text{top}}(\theta) + 1.2/1.75J_c^{\text{bottom}}(\theta)]$ . As we did not measure the top and bottom layers separately for the *same* link, a direct (unnormalized) comparison was not possible.

$J_c(H\parallel ab)/J_c(H\parallel c) \sim 4$ . The inset of Fig. 4 presents the full thickness, measured  $J_c(\theta, 65 \text{ K}, 3 \text{ T})$  dependence, and that calculated from the thickness-weighted sum of the individual layers  $[0.55/1.75J_c^{\text{top}}(\theta) + 1.2/1.75J_c^{\text{bottom}}(\theta)]$ . The shapes of the two curves in the inset are nearly identical, demonstrating that the  $J_c$  anisotropy of a MOD-grown composite film could be tuned by varying the thicknesses and pinning structures of the layers within the composite. The results at other fields (1 T, 3 T, and 5 T) and 77 K were similar.

When a pinning structure is incorporated into a HTS film, the result is not necessarily a linear superposition of the pinning properties of the new structure and previously existing pinning structures, since chemistry changes might alter pre-existing structures or dimensional vortex-vortex and vortex-pin interactions could be greatly changed. In this work, the fact that the anisotropy of the two individual layers contributes additively to the anisotropy of the overall composite strongly suggests that the vortex pinning within each layer occurs independently of the other. One interpretation is that both layers within the composite are in the strong three-dimensional pinning limit, where flux lines are decoupled into short segments extending between strong pins spaced much closer than each layer thickness, consistent with the spacing of the Y124 intergrowths and  $\text{Dy}_2\text{O}_3$  particles shown in Fig. 2.<sup>22,23</sup> However, the strong three-dimensional pinning should result in a flat thickness dependence of  $J_c$ , whereas we found a 40% increase in  $J_c$  as the film was thinned (inset of Fig. 1), indicating that the thickness-dependent microstructural degradation effects also play a significant role, as is common in MOD conductors.<sup>20</sup> Cross-sectional TEM and electron backscatter diffraction of each layer (not shown) revealed a reduced grain alignment of the top layer relative to the bottom layer.

In summary, we have presented a detailed study of the critical current anisotropy as a function of thickness of a composite bilayer film grown by MOD with different dominant pinning mechanisms in each layer. Through cross sectional TEM and by isolating each layer individually for

transport measurement, we revealed that the pinning properties and microstructure of each defect type are preserved within the bilayer, and that the overall  $J_c$  and its anisotropy is a thickness-weighted sum of the individual layers. These results suggest that a very high degree of tunability is possible in YBCO films by varying the number of layers and the defect type within each layer in a composite film.

This work was funded by the Department of Energy and by the Air Force Office of Scientific Research.

- <sup>1</sup>D. Larbalestier, A. Gurevich, D. M. Feldmann, and A. Polyanskii, *Nature (London)* **414**, 368 (2001).
- <sup>2</sup>J. L. MacManus-Driscoll, S. R. Foltyn, Q. X. Jia, H. Wang, A. Serquis, L. Civale, B. Maiorov, M. E. Hawley, M. P. Maley, and D. E. Peterson, *Nat. Mater.* **3**, 439 (2004).
- <sup>3</sup>L. Civale, B. Maiorov, A. Serquis, S. R. Foltyn, Q. X. Jia, P. N. Arendt, H. Wang, J. O. Willis, J. Y. Coulter, T. G. Holesinger, J. L. MacManus-Driscoll, M. W. Rupich, W. Zhang, and X. Li, *Physica C* **412-414**, 976 (2004).
- <sup>4</sup>H. Wang, S. R. Foltyn, P. N. Arendt, Q. X. Jia, and X. Zhang, *Physica C* **444**, 1 (2006).
- <sup>5</sup>B. Dam, J. M. Huijbregtse, F. C. Klaassen, R. C. F. van der Geest, G. Doornbos, J. H. Rector, A. M. Testa, S. Freisem, J. C. Martinez, B. Stauble-Pumpin, and R. Griessen, *Nature (London)* **399**, 439 (1999).
- <sup>6</sup>D. M. Feldmann, T. G. Holesinger, C. Cantoni, R. Feenstra, N. A. Nelson, D. C. Larbalestier, D. T. Verebelyi, X. Li, and M. Rupich, *J. Mater. Res.* **21**, 923 (2006).
- <sup>7</sup>T. Haugan, P. N. Barnes, R. Wheeler, F. Meisenkothen, and M. Sumption, *Nature (London)* **430**, 867 (2004).
- <sup>8</sup>T. Aytug, M. Paranthaman, A. A. Gapud, S. Kang, H. M. Christen, K. J. Leonard, P. M. Martin, J. R. Thompson, D. K. Christen, R. Meng, I. Rusakova, C. W. Chu, and T. H. Johansen, *J. Appl. Phys.* **98**, 114309 (2005).
- <sup>9</sup>R. L. S. Emergo, J. Z. Wu, T. J. Haugan, and P. N. Barnes, *Appl. Phys. Lett.* **87**, 232503 (2005).
- <sup>10</sup>K. Matsumoto, T. Horide, K. Osamura, M. Mukaida, Y. Yoshida, A. Ichinose, and S. Horii, *Physica C* **412-414**, 1267 (2004).
- <sup>11</sup>P. C. McIntyre, M. J. Cima, and M. F. Ng, *J. Appl. Phys.* **68**, 4183 (1990).
- <sup>12</sup>M. W. Rupich, D. T. Verebelyi, W. Zhang, T. Kodenkandath, and X. P. Li, *MRS Bull.* **29**, 572 (2004).
- <sup>13</sup>T. G. Holesinger, B. Maiorov, J. Y. Coulter, L. Civale, X. Li, W. Zhang, Y. Huang, T. Kodenkandath, and M. W. Rupich, *IEEE Trans. Appl. Supercond.* (to be published).
- <sup>14</sup>T. G. Holesinger, L. Civale, B. Maiorov, D. M. Feldmann, Y. Coulter, D. Miller, V. Maroni, D. C. Larbalestier, R. Feenstra, X. Li, Y. Huang, T. Kodenkandath, W. Zhang, M. Rupich, and A. Malozemoff, *Adv. Mater.* (to be published).
- <sup>15</sup>N. Long, N. Strickland, B. Chapman, N. Ross, J. Xia, X. Li, W. Zhang, T. Kodenkandath, Y. Huang, and M. Rupich, *Supercond. Sci. Technol.* **18**, S405 (2005).
- <sup>16</sup>E. D. Specht, A. Goyal, J. Li, P. M. Martin, X. Li, and M. W. Rupich, *Appl. Phys. Lett.* **89**, 162510 (2006).
- <sup>17</sup>M. W. Rupich, D. Miller, T. G. Holesinger, and D. M. Feldmann, *Proceedings of the 2006 Department of Energy Superconductivity Program Peer Review*, Washington, D.C. (unpublished).
- <sup>18</sup>A. Goyal, S. X. Ren, E. D. Specht, D. M. Kroeger, R. Feenstra, D. Norton, M. Paranthaman, D. F. Lee, and D. K. Christen, *Micron* **30**, 463 (1999).
- <sup>19</sup>D. M. Feldmann, D. C. Larbalestier, R. Feenstra, A. A. Gapud, J. D. Budai, T. G. Holesinger, and P. N. Arendt, *Appl. Phys. Lett.* **83**, 3951 (2003).
- <sup>20</sup>S. I. Kim, A. Gurevich, X. Song, X. Li, W. Zhang, T. Kodenkandath, M. W. Rupich, T. G. Holesinger, and D. C. Larbalestier, *Supercond. Sci. Technol.* **19**, 968 (2006).
- <sup>21</sup>X. Li, M. W. Rupich, T. Kodenkandath, Y. Huang, W. Zhang, E. Siegal, D. T. Verebelyi, U. Schoop, N. Nguyen, C. Thieme, Z. Chen, D. M. Feldmann, D. C. Larbalestier, T. G. Holesinger, L. Civale, Q. X. Jia, V. Maroni, and M. V. Rane, *IEEE Trans. Appl. Supercond.* (to be published).
- <sup>22</sup>S. I. Kim, D. M. Feldmann, D. T. Verebelyi, C. Thieme, W. Zhang, A. A. Polyanskii, and D. C. Larbalestier, *Phys. Rev. B* **71**, 104501 (2005).
- <sup>23</sup>Z. Chen, D. M. Feldmann, X. Song, S. I. Kim, A. Gurevich, J. L. Reeves, Y. Y. Xie, V. Selvamanickam, and D. C. Larbalestier, *Supercond. Sci. Technol.* (to be published).